

Radiological Detection and Assessment of Tumor Response

TOBIAS F. JAKOBS

CONTENTS

9.1	Introduction	93
9.2	Methods of Assessment	94
9.2.1	WHO and RECIST	94
9.2.1.1	Advantages of WHO and RECIST	94
9.2.1.2	Disadvantages of WHO and RECIST	95
9.2.2	Alternative Measurements	96
9.3	Imaging	97
9.3.1	Dual-Modality Positron Emission Tomography/Computed Tomography (PET-CT)	97
9.3.1.1	Proposal for a PET-CT Scan Protocol	98
9.3.2	Whole-Body Magnetic Resonance Imaging (WB-MRI)	98
9.3.2.1	Technical Requirements	98
9.3.2.2	MRI Sequences for Whole-Body Imaging	99
9.3.2.3	Proposal for a Whole-Body MR Scan Protocol	99
9.4	Discussion	100
9.4.1	Detection of Liver Metastases	100
9.4.2	Follow-Up of Recurrent Metastatic Disease	100
9.4.3	PET or PET-CT	101
9.4.4	What Does MRI Add?	101
9.5	Outlook	104
9.6	Conclusion	104
	References	104

9.1

Introduction

The liver is the most common site of metastatic spread in malignancies. In autopsy studies the incidence of hepatic metastases is up to 100%, depending on the primary tumor. Even if this fact represents the final status of a malignancy, about half of all patients dying from a malignant disease will have apparent hepatic metastases. The risk of developing hepatic metastases varies widely among different types of primary malignancy.

In the case of predominant metastatic spread to the liver, the long term survival is mostly determined by the extent of this particular tumor manifestation.

Presently, numerous palliative hepatic-directed therapies are available for the treatment of non-resectable liver tumors, including conformal radiation therapy, ^{90}Y microsphere brachytherapy, hepatic arterial infusion chemotherapy, transarterial chemoembolization, radiofrequency ablation and combinations of these treatments.

Therefore, reliable tumor assessment with high diagnostic accuracy is a fundamental precondition for selecting the appropriate therapy and is indispensable for assessing patient's response to treatment. Consequently, applied diagnostic methods should be as sensitive and specific as possible. An effective treatment of hepatic tumors is crucial for improved survival outcome. So far, a complete evaluation of tumor spread in patients with advanced cancer requires various imaging procedures, such as computed tomography (CT), magnetic resonance imaging (MRI), ultrasound, radiography, radiographic skeletal survey and bone scintigraphy. This approach is time-consuming, inconvenient for the patient, expensive and can miss lesions outside the fields of study.

Recently, whole-body imaging modalities like dual-modality positron emission tomography/computed tomography (PET-CT) and whole-body MRI have been introduced and offer a complete head-to-toe coverage of the patient in a single examination with an accurate and sensitive detection of tumor spread [1, 33, 40].

9.2

Methods of Assessment

The RECIST (Response Evaluation Criteria in Solid Tumors) [46] and the WHO (World Health Organisation) method [28] define standard measurement methods for converting visual image observations into a quantitative and statistically tractable framework for measuring tumor size response to therapy. Although the WHO method was first developed for radiography and computed tomography (CT), it was modified in the RECIST publication (dated 2000) to make measurement practices procedurally more consistent across multiple trials and accommodate improvements in CT and MRI technology. Both methods offer simple approaches to determining anatomic size and time-evolving lesion-changes during treatment as an indicator of response. Each method uses a pragmatically simplistic technique dependent on observer judgment of lesion boundaries. WHO defines its tumor measurement by summing a group of individual masses, each lesion of which is assessed by the cross product of its greatest diameter and largest perpendicular diameter. RECIST was designed to be sufficiently aligned with WHO practices such that no major discrepancy would occur in the concept of partial response between the old and new guidelines. It also provides a clearly understandable look-up table defining response classification (Table 9.1).

9.2.1 WHO and RECIST

Once target lesions (up to five per organ) are measured using either single linear summation (RECIST) or the bilinear product approach (WHO), the results are subsequently assigned to response-defined categories of complete response (CR), partial response (PR), stable disease (SD) and progressive disease (PD). By somewhat arbitrary decision making, RECIST defined PR as a more than 30% linear decrease of the linear sums of the target lesions (thus, by extrapolation, implying a 65% volumetric decrease) and PD as a more than 20% increase (implying a 73% volumetric increase). This contrasted with WHO criteria, in which those boundaries are set volumetrically at 65% and 40%, respectively.

9.2.1.1 Advantages of WHO and RECIST

As a simply implemented procedure, RECIST has both its advocates and critics. Publications both supportive and critical can be cited in the scientific literature [15, 26, 31]. RECIST and WHO have their devotees as easily understood methods that allow simple ruler analysis of printed films as well as workstation use of electronic calipers to produce comprehensible results. Clinical imaging usually provides correlative or mostly secondary trial end points, so RECIST and WHO criteria provide pragmatically adequate tools that satisfy a non-critical role relative to other data and clinical outcome that take primacy. They are accommodating of a variety of imaging acquisition circumstances and place minimal added demand on routine clinical practices. In sum, they have been perceived as simple tools adequate to imaging's supportive role. To date, few widely available alternatives exist that are as easily executed or of provably greater benefit to jus-

Table 9.1. RECIST criteria offer a simplified, conservative, extraction of imaging data for wide application in clinical trials. They presume that linear measures are an adequate substitute for 2D methods and register four response categories

Category	Imaging finding
CR (complete response)	Disappearance of all target lesions
PR (partial response)	30% Decrease in the sum of the longest diameter of target lesions
SD (stable disease)	Small changes that do not meet above criteria
PD (progressive disease)	20% Increase in the sum of the longest diameter of target lesions

tify further expense, time demands, or operational complexity [49].

9.2.1.2

Disadvantages of WHO and RECIST

As RECIST was framed in the context of individual slices, the research community is currently re-exploring the obvious gaps in both RECIST and WHO criteria, which admittedly were constrained by the limits of earlier technology. To list the most obvious shortcomings, neither linear nor bilinear based methods address intratumor heterogeneity and its change over time, as it might occur after tumor targeted therapy (e.g. ^{90}Y microsphere therapy, radiofrequency ablation etc.), nor do they reflect appropriate measures for tumor metabolism

(Fig. 9.1). They do not incorporate multi-slice integrated understanding, register information about time-sequence change of shape or morphologic complexity, or address statistical uncertainties arising from low-intensity lesion edges. The techniques do not provide methodological distinctions between tumors of inherently high contrast compared with their surrounding tissue (e.g. lung), nor do they prescribe specific approaches to the use of contrast materials usually needed to enhance intra-abdominal soft tissue findings [16]. Most importantly, little attention was paid in the guidelines to inconsistencies inherent in the expert observer. The reader makes his/her measurements unassisted by anything other than the most rudimentary form of image-processing technology (often simply the use of electronic calipers on a workstation display). Nei-

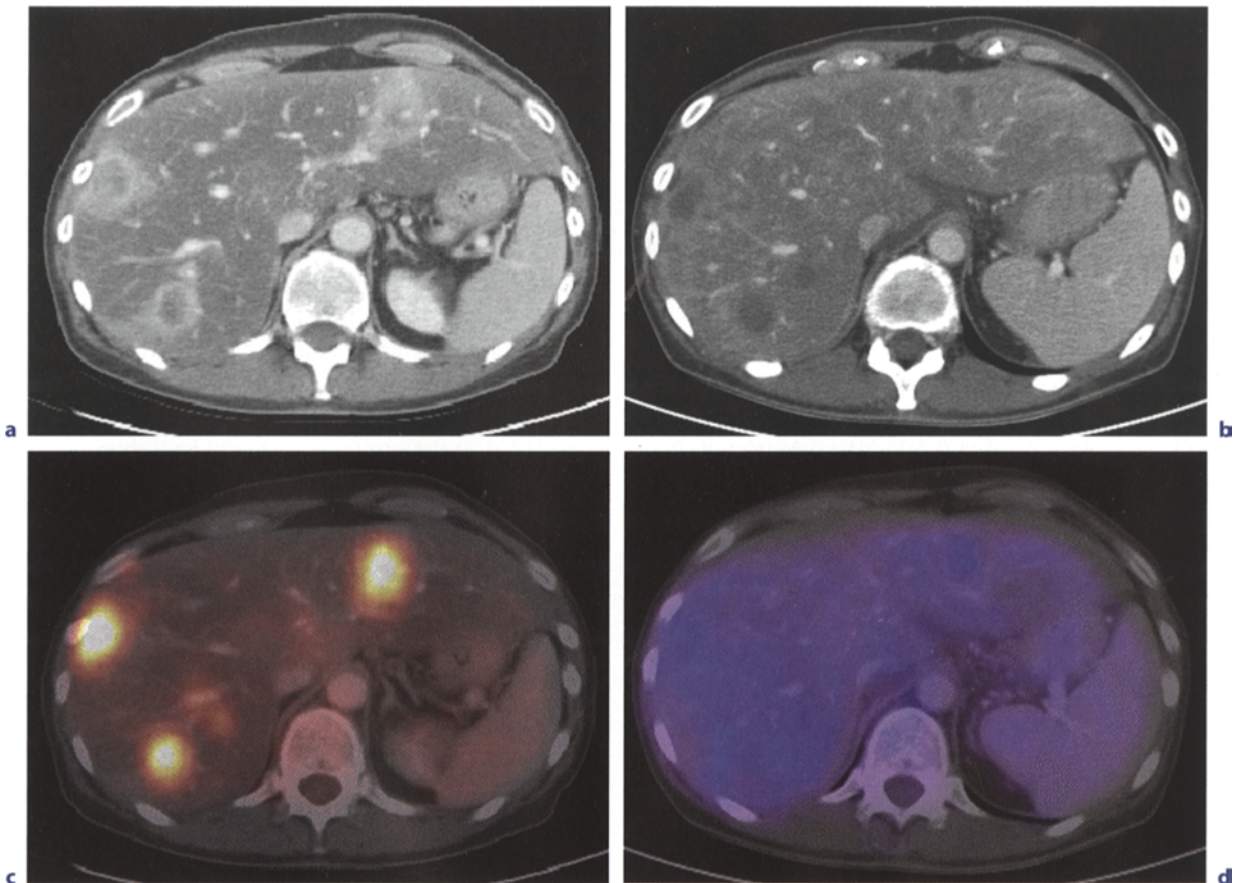


Fig. 9.1a–d. A 47-year-old female patient with hepatic metastases from pancreatic cancer. Contrast enhanced CT (a) shows multiple liver lesions with rim enhancement. The corresponding fused PET-CT image (c) demonstrates high FDG-uptake due to increased tumor metabolism. The CT scan 4 months after radioembolization (b) delineates hypovascular tumor lesions without significant change concerning their size. According to RECIST this displays the response category “stable disease”. The fused PET-CT image (d) proves that there is no increased tumor metabolism in the area of the former metastases, therefore indicating that this result represents a “complete remission”

ther RECIST nor WHO provide especially rigorous guidance on the subject of observer variability aside from recommending review panels and independent observers. Disagreement among observers has been noted to be as high as 15%–40% in these contexts and may not be ideally remedied by consensus [5]. Besides providing only nominal guidance on slice thickness, RECIST does not address at any length image acquisition components that inevitably result in significant lesion contrast differences within and between studies, such as lack of uniformity of machine settings for kVp (peak kilovolts) and mAs (milliamperere seconds) in CT, and pulse sequences in MRI. As a simply adoptable, widely applicable method, posing no impediment to accrual from a wide range of CT and MRI sites, RECIST has served a useful historic purpose in grouping image data into the rough four-group response classifications (CR, PR, SD, PD). But since diameter measurements are best determined on smoothly shaped, distinct tumor boundaries, an ideal circumstance encountered infrequently, measurement variability inherent in such judgments is not adequately reflected in the recorded data. Tumors with irregular or diffuse boundaries pose the most significant challenge to data extraction and are highly observer dependent. Indeed, tumor boundary distinctiveness varies on a disease- or organ-specific basis. Observer recognition of boundaries may be further complicated by necrosis-caused internal heterogeneity that permeates the tumor or expresses itself asymmetrically on the lesion edge. Especially in the liver, tumor boundary sharpness in both CT and MRI may be enhanced by injection of contrast agents. But contrast agent pharmacokinetics are variable, and image acquisition routines are often compromised because they are usually prescribed by time from contrast administration, rather than the more definitive, but harder to obtain, contrast arrival time within specific organs.

9.2.2

Alternative Measurements

Technological advances in tomographic scanners, both CT and MRI, have been unrelenting. In the span of less than a decade, CT scanners have advanced from single-detector arrays that scanned body segments in more than a minute (thus nearly always subject to motion artifacts), to present-day instruments with two simultaneous X-ray sources,

64 detector arrays, submillimeter voxel resolution and motion-resistant body-segment acquisition speed of less than 10 s. These have been matched by post-processing display improvements that provide real-time visualization from any arbitrary (multiplanar) view. Image processing based on voxel intensity neighborhoods is sufficiently commonplace that near immediate three-dimensional display of selected organs or the entire body are an expected part of conventional image reconstruction routines. In reality though, the advantages of tomography that offers submillimeter, isovolumetric imaging has yet to be fully absorbed into routine diagnostic practice, not to mention exploited for its potential to enhance the measurement processes in cancer patients' follow-up. Most clinical trial tomographic imaging is still conducted at slice thicknesses of 5 or 7 mm in the intuitive conviction that those parameters are sufficient for the task required and for the convenience of the observer, who does not wish to be burdened by a vast number of images.

The availability of potentially more accurate and reproducible tumor volume data could motivate a re-examination of the foundations of the established categories of CR, PR, SD, and PD. RECIST, as it does not specify whole-body imaging at the time of each evaluation which may register conclusions that fail to account for non-imaged parts of the body. Assignment to CR, PR, etc. in following an abdominal malignancy could be misleading if there is not apparent presence of non-imaged metastases in lung or brain when those body regions were not prescribed in the protocol. Imaging techniques that are whole-body oriented, like PET, combined PET-CT and whole-body MRI, thus have advantages from this perspective. RECIST addresses this possibility by acknowledging that events that can occur in the non-measurable targets, such as the growth of non-measurable lesions or the appearance of new lesions despite unchanged size of target lesions. In these circumstances RECIST mandates a classification shift from SD to PD. But these body regions must first be imaged in order to trigger those rules. Image-processing algorithms, mathematically and globally operating in true three-dimensional data space, as exemplified by techniques known as auto-contouring, region growing, nearest neighbor, annealing, gradient following, water shed and statistical modelling, have been effective in a variety of scientific fields. They hold sufficient promise to deserve an opportunity to contribute to oncology. It is evident from image processing's operational sphere that it is

powered by mathematical approaches far exceeding the innate comprehension capacity of human observers. These sophisticated tools have already made key contributions to advances in medical image reconstruction and are the cornerstone of the remarkable anatomic detail we usually take for granted in our clinical environment.

Efforts to develop reproducible methods for measuring volumes of infiltrative tumors that lack clear margins, already recognized as a serious problem for linear and two-dimensional area measurement. Pathologic or histologic validation is unlikely to be clinically practicable. Given that ultimate validation is difficult, the mere task of generating a convincing test, whether precise or statistical, to compare alternative algorithms poses a challenge. In the past it has been convenient to accept expert consensus despite the obvious flaw of relying on human opinion as a gold standard.

Promising recent developments for validation might be inferred from data derived from co-registration of MRI and CT images or PET-CT, which permit three-dimensional anatomic CT to be combined with simultaneous tumor metabolic activity from the PET in fused, spatially registered images. This might be a first step in a path toward more rigorous validation.

9.3

Imaging

In heavily pretreated patients with known malignancy, possible further therapeutic strategies depend on the stage of disease, liver involvement and whether multiple organ systems have been affected. In the past, patients had to undergo a variety of different diagnostic procedures to achieve a comprehensive staging or screening, including imaging studies such as ultrasonography, CT, MRI, PET and X-ray examinations. The combination of these procedures is often time-consuming and inconvenient for the patient. Thus, a single imaging examination providing information of different organ systems (ideally of the entire body) would be of great interest.

Due to the mentioned limitations of conventional tomographic imaging (CT and MRI) in assessing the tumor response after tumor targeted therapy like ^{90}Y local radiation therapy, some studies have suggested that PET or PET-CT represent valuable

tools in assessing tumor response [41, 55–57]. As described earlier, anatomic imaging by CT or MRI is more or less insensitive in correctly determining tumor response by simply measuring the change in diameters because of the presence of central necrosis, edema, cystic changes and hemorrhage. Given the lack of reliability of tumor markers (where applicable) in the presence of extrahepatic tumor manifestation, PET appears to be an excellent adjunct to define response after regional treatment of liver metastases [3].

9.3.1

Dual-Modality Positron Emission Tomography/Computed Tomography (PET-CT)

Whole-body PET using [^{18}F]-fluoro-2-deoxy-D-glucose (FDG) is an imaging modality enabling detection of cancerous disease by tracing increased accumulation of FDG in tumor tissue. The introduction of combined PET-CT scanners has made a new modality available for whole-body imaging, combining the functional data of PET with the detailed anatomical information of CT imaging in a single examination [6].

FDG-PET provides a functional metabolic map of glucose uptake in the whole body. FDG is a glucose analogue that is labeled with the positron emitting radioisotope fluorine-18 that is produced by a cyclotron. The resulting radiopharmaceutical agent F-18 FDG is taken up by metabolically active tumor cells using facilitated transport similar to that used by glucose. The rate of uptake of FDG by tumor cells is proportional to their metabolic activity. Since FDG is a radiopharmaceutical analog of glucose, it also undergoes phosphorylation to form FDG-6-phosphate like glucose. However, unlike glucose, it does not undergo further metabolism, thereby becoming “trapped” in metabolically active cells [17]. In general, PET is limited by poor anatomic detail, and therefore, anatomical correlation with some other form of imaging, such as CT, is desirable for differentiating normal from abnormal radiotracer uptake and accurate lesion localization.

First study results indicate that a fusion of both modalities (PET and CT) improves diagnostic accuracy as well as lesion localization and report promising results for the staging of different oncological diseases compared to PET and CT alone [21, 32]. The total standard uptake value (SUV) of the entire axial slices of the liver as well as of the individual lesion

correlated well with the laboratory and tomographic imaging results [56]. However, PET-CT in some cases holds a risk of diagnostic misinterpretation, e.g. due to increased FDG-uptake in muscle or fat tissue, reduced spatial resolution or incorrect lesion localization caused by an inadequate fusion of the PET and CT data due to breathing artifacts.

9.3.1.1

Proposal for a PET-CT Scan Protocol

Before performing the PET-CT scan patients have to have been fasting for at least 6 h to keep blood sugar levels below 120 mg/dl. After an intravenous injection of Furosemide and Butylscopolamin (20 mg each), the application of approximately 370 MBq [¹⁸F]-fluoro-2-deoxy-D-glucose (FDG) is followed. At 60 min after the tracer application, a low dose-CT scan is performed from the skull base to the proximal femur for attenuation correction. Using a 3D-mode (144 × 144 matrix) the emission scans are then conducted with 3 min per bed position (FOV 10 cm). For a whole-body examination an average of 12 positions is needed. After the emission scan, patients have a diagnostic spiral-CT scan (40 mA, 120 kV, collimation 2 × 5 mm, pitch 1.5; using e.g. a two-detector row PET-CT system) covering thorax, abdomen and pelvis with 120 ml of nonionic iodinated i.v. contrast agent in the venous phase (70–80 s delay). Multiplanar reconstructions are performed on the diagnostic CT data set. Using the emission data, a reconstruction of the PET data with and without attenuation correction (Ramla-3D) and a reorientation in axial, sagittal and coronal direction is followed. Finally, with the use of dedicated software the PET and CT data are fused.

9.3.2

Whole-Body Magnetic Resonance Imaging (WB-MRI)

9.3.2.1

Technical Requirements

Whole-body MRI has not been used in routine clinical care either because of extensively long examination times when diagnostic-quality sequences are employed, or because of inferior quality when fast sequences are utilized. To overcome these problems, different strategies have been explored. One approach has been the implementation of a slid-

ing table platform that enables data acquisition of different anatomical regions in rapid succession [4]. Signal reception can be accomplished using posteriorly-located spine coils (integrated in the patient table) and an anteriorly positioned torso phased-array coil, which remains fixed to the stationary patient table in the isocenter of the magnet. Hence, data acquisition can be performed with the same stationary coil set. A rolling table platform has been successfully employed for the detection of bone metastases, parenchymal metastases including hepatic, cerebral, and lung metastases [23]. Other technological advances provide MRI systems with multiple input channels, which allow the simultaneous use of specialized surface coils [39]. A combination of coils, for example, a head coil with two or more phased-array body coils, can be employed simultaneously. Thus, high-resolution images of multiple regions of the body can be acquired without the need for coil repositioning. Automatic table motion can acquire a total scan range of over 200 cm in the z-axis. Beyond the technical improvements in system hardware, concurrent developments have been made in MRI sequence protocols and imaging techniques. An important innovation is the use of fat suppressed three-dimensional (3D) gradient echo (GRE) sequences with nearly isotropic resolution, which has been developed for imaging of parenchymal organs [24, 35]. These 3D data sets can be acquired within a single breath-hold and provide excellent image quality. Furthermore, 3D data also offers the advantage of multiplanar reconstructions. In conjunction with rapid table motion, these T1-weighted (T1w) sequences permit dynamic imaging of various parenchymal organs after a single intravenous injection of paramagnetic contrast agents. Further improvement of whole-body MRI is achieved by using parallel acquisition techniques (PAT). These techniques allow data acquisition with either increased spatial resolution or shorter acquisition time, or a combination of both [14, 19]. Combining a high number of surface coil elements and receiver channels now enables PAT imaging in all three spatial directions. In principal, the image reconstruction can be facilitated by two different algorithms: either by calculation of the missing k-space lines before Fourier transformation (SMASH or GRAPPA) or by later fusion of the generated incomplete images (SENSE) [14, 34]. Thus, the combined effect of hardware and sequence advances has allowed whole-body MRI to be performed more rapidly while maintaining diagnostic image quality.

9.3.2.2

MRI Sequences for Whole-Body Imaging

Examination protocols should be tailored to specific clinical circumstances. However, all whole-body protocols should include gadolinium enhanced T1w 3D GRE sequences of all different organ systems, and especially the liver for evaluation of the efficacy of regional tumor therapy. Whole-body MRI using only unenhanced imaging would substantially shorten examination times, but diagnostic accuracy would be substantially reduced. After contrast administration, data collection should be started in the abdomen with an arterial, portal venous and late venous contrast phase of the liver. With this type of protocol, high sensitivity and specificity for focal liver lesions can be achieved. Moreover, anti-tumoral effects after liver-directed, minimal invasive therapies can be assessed. As compared to PET/CT, whole-body MRI has a higher sensitivity in the detection of liver metastases and primary liver tumors. Whole-body MRI is also definitely superior in the detection of skeletal and brain metastases. In the assessment of lymph node involvement, on the other hand, PET/CT is most accurate.

9.3.2.3

Proposal for a Whole-Body MR Scan Protocol

First, coronal STIR (short tau inversion recovery)-sequences (TR 5620/TE 92, 5-mm slices, matrix

384 × 269), at five levels (head, neck, pelvis, thighs and lower leg), as well as thorax/abdomen (TR 3380/TE 101) in breath-hold technique with prospective 2D navigation correction of the inspiration phase (PACE, prospective acquisition correction) are acquired. Using PAT, image acquisition can be completed within an acceptable time with a 1.8 × 1.3 mm in-plane resolution. Additionally, the lung is examined in axial orientation with STIR (TR 3800/TE 100, 6-mm slices, matrix 320 × 156) and HASTE sequences (TR 1100/TE 27). After a navigator-triggered “free-breathing” T2w fat saturated SE scan of the liver (TR 2010/TE 101, 6-mm slices, matrix 320 × 240) the five body levels are examined with T1w SE sequences (TR 79/TE 12, 5-mm slices, matrix 448 × 385; thorax/abdomen TR 400/TE 8.2), followed by T1w (TR 849/TE 11, SD 3 mm, matrix 384 × 384) and STIR imaging (TR 5700/TE 59) of the spine in sagittal orientation. After application of gadolinium-DTPA (3 ml/s; 0.2 mmol/kg) and saline flushing (20 ml), axial dynamic (arterial, portal venous, late venous phase) liver scans are performed (TR 4.38/TE 1.61, 3-mm slices), as well as axial T1w and T2w imaging (TR 635/TE 17, 5-mm slices, matrix 320 × 240 and TR 1420/TE 109, matrix 512 × 250) of the brain. The last examination step consists of a fat saturated T1w GRE sequence of the whole abdomen in axial orientation (TR 179/TE 3.33, matrix 320 × 193, 6-mm slices). Table 9.2 gives an overview of the scan protocol. A PAT factor of 3 is

Table 9.2. Overview of a possible scan protocol applied to a whole-body magnetic resonance scanner with 32-receiver channels. Total scan time approximately 55 min

Localization	Whole-Body MRI protocol					
	STIR cor		T1 cor			T1 +con, T2 ax skull
	STIR cor	HASTE/STIR cor + ax lung	T1 cor	T1+STIR upper spine		T1 fs ax + con abdomen
	STIR cor	T2 liver	T1 cor	T1+STIR lower spine	3D-VIBE upper abdomen	
	STIR cor		T1 cor			
	STIR cor		T1 cor			
	0 min	→	→	→	→	→

used for the coronal T1w/STIR whole-body imaging apart from the lower leg. A PAT-factor of 2 is used for axial imaging of brain, lung and abdomen, as well as for the sagittal scans of the spine and for the coronal scans of the lower leg.

9.4

Discussion

9.4.1

Detection of Liver Metastases

Imaging plays a major role in detecting and follow-up of metastatic disease in the liver, which strongly influences the treatment strategy. Contrast enhanced CT has been reported as the most sensitive test for the detection of hepatic metastases. However, it has a considerable rate of false-positive findings, lowering the positive predictive value [29, 43]. False-positive results from FDG-PET in the liver are rare and occur primarily in hepatic abscesses. Delbeke et al. [9] reported a lower sensitivity (91% versus 97%) but higher specificity (95% versus 50%) for FDG-PET resulting in a superior overall diagnostic accuracy compared to contrast enhanced CT. In the study of Topal et al. [47], PET was shown to be capable of detecting liver metastases with 99% sensitivity. Several studies have compared the accuracy of FDG-PET and CT in the detection of hepatic metastases [2, 7, 30]. Overall, FDG-PET was more accurate than CT. Ogunbiyi et al. [30] reported high sensitivity (95%) and specificity (100%) of FDG-PET for detecting liver metastases. In their study the sensitivity and specificity of CT were 74% and 85%, respectively. In a meta-analysis, Kinkel et al. [18] compared ultrasonography, CT, and MRI and FDG-PET in the detection of hepatic metastases from colorectal, gastric, and esophageal cancer. In this study, the sensitivity of the modalities with specificity higher than 85% was 55% for ultrasonography, 72% for CT, 76% for MRI, and 90% for FDG-PET.

Nevertheless, controversy still remains over the role of FDG-PET in the detection and follow-up of liver tumors. In several articles comparing PET and CT, there were potential sources of bias that could benefit PET over CT including the interval between CT and PET, unequal skill in test performance, variations in CT technology and bias in test interpretation. Recently, Truant et al. [50] reported equivalent

sensitivities for FDG-PET and CT for the detection of colorectal liver metastases (76%). Concerning the comparison with MRI, Yang et al. [58] found no significant difference in the detection of liver metastases with gadolinium chelate-enhanced liver MRI and FDG-PET. In the study of Bohm et al. [7] comparing FDG-PET with other cross-sectional anatomical imaging techniques, FDG-PET performed better than sonography and CT. However, gadolinium-chelate enhanced MRI had comparable results. In this study, the sensitivity and positive predictive value of PET for hepatic lesions from colorectal cancer were 94% and 99%, respectively, compared with 86% and 100% for abdominal sonography; 88% and 98% for CT; and 91% and 100% for MRI. Recently, Sahani et al. [38] compared mangafodipir trisodium-enhanced liver MRI and FDG-PET for the detection of hepatic metastases from the adenocarcinoma of the colon and pancreas and found accuracies of 97.1% for MRI and 85.3% for FDG-PET. However, apart from its high sensitivity in the detection of hepatic metastatic lesions, FDG-PET provides a survey of the whole body for metastatic disease. Sahani et al. [38] reported that FDG-PET identified extrahepatic disease in nine of the 34 patients involved in their study. In the study of Arulampalam et al. [2] FDG-PET had an overall sensitivity of 100% and an overall specificity of 91% for intra- and extrahepatic metastatic disease. The overall sensitivity and specificity of CT were 47% and 91%, respectively. FDG-PET might be not far superior to CT or MRI in the detection of hepatic metastases, but it surely adds to the decision making power of the oncologist and interventional radiologist and may impact on the management of many patients due to its high sensitivity for intrahepatic and extrahepatic metastatic disease.

9.4.2

Follow-Up of Recurrent Metastatic Disease

The measurement of tumor markers (where applicable) may be used to monitor recurrence, with a sensitivity of 59% and a specificity of 84% [10]. In addition to its low sensitivity, tumor markers do not enable localization of recurrent lesions. CT has been the established imaging modality to demonstrate recurrent hepatic metastases or tumor progression after regional therapy. However, CT is unable to detect hepatic lesions in up to 7% of patients and underestimates the number of lobes involved in up to 33% of patients [10]. Selzner et al. [41] compared CT and

FDG-PET in 76 patients evaluated for liver resection for metastatic colorectal cancer. CT and FDG-PET provided comparable findings for the detection of intrahepatic metastases with a sensitivity of 95% and 91%, respectively. However, the specificity of FDG-PET (100%) was significantly superior to that of CT (50%) in establishing the diagnosis of intrahepatic recurrences in patients with prior treatment. Selzner et al. [41] reported that in half of the patients with local recurrences in the liver, CT provided no or inconclusive information; whereas all recurrent metastases exhibited positive FDG-uptake in their study. In fact, this finding is not surprising because it is well known that differentiation of postoperative or postinterventional changes after regional tumor therapy and tumor recurrence based on morphologic findings alone is difficult [41]. Since PET has the ability to give information about the metabolic activity of a particular tissue, it has great potential to predict response to systemic chemotherapy or regional therapy much earlier than with morphological imaging methods which require evidence of morphological changes that may take some weeks [51].

Apart from systemic chemotherapy, hepatic metastases can also be treated with regional therapy. Various procedures such as selective chemoembolization, radiofrequency ablation, cryoablation, alcohol ablation and ^{90}Y microsphere therapy have been investigated. Vitola et al. [53] and Torizuka et al. [48] showed that FDG-uptake decreases in responding lesions after chemoembolization and the presence of residual uptake in some lesions can help in guiding further therapy. Langenhoff et al. [20] have prospectively monitored 23 patients with liver metastases following radiofrequency ablation and cryoablation. At 3 weeks following therapy, 51 of 56 (91%) metastases became FDG negative, and no recurrence was detected during the follow-up period of 16 months. Wong et al. [56] compared PET, CT or MRI and serum levels of CEA to monitor the therapeutic response of hepatic metastases to ^{90}Y microsphere brachytherapy. They found significant differences between PET, CT and MRI; and the changes in FDG-uptake correlated better with the serum levels of CEA.

9.4.3

PET or PET-CT

PET and PET-CT have changed the management of patients with liver malignancies as a result of their

enhanced ability to detect recurrent or metastatic lesions compared with CT alone [27, 36]. Despite its limitations, PET has also proved to be more accurate than CT in detecting recurrent liver metastases [13, 52]. The inability to provide detailed anatomic information is, however, an important limitation of PET imaging. It is impossible, for example, to assess the proximity of liver lesions to important anatomical structures such as vena cava, portal vein, or biliary duct [18]. Thus, it is frequently necessary that PET imaging be complemented by other studies such as CT or MRI [37]. PET-CT is a recently developed integrated imaging modality that combines CT (anatomical information) and PET (functional information). Compared to PET alone, PET-CT greatly improves confidence concerning lesion location [8]. In a study comparing PET alone with PET-CT, the number of lesions with uncertain location was reduced by 55% (from 42 to 19). Moreover, the number of equivocal and probable lesion characterizations was reduced by 50% (from 50 to 25). Confidence in lesion localization and characterization are linked with each other, as better localization of a lesion probably also improves the accuracy of its characterization as benign or malignant, leading to fewer equivocal lesions and fewer lesions that are considered probably benign or probably malignant.

9.4.4

What Does MRI Add?

Initial studies describing whole-body MRI focused on the detection of osseous metastases in patients with primary malignancies that had a high likelihood to spread to the skeletal system [12, 44]. Bone scintigraphy served as the reference standard in these studies. Dedicated MRI had been found to be more accurate in the detection of bone metastases compared to scintigraphy. In the detection of skeletal metastases, distinct regional advantages and disadvantages were observed for both skeletal scintigraphy and whole-body MRI. Scintigraphy proved more sensitive in the assessment of metastases to the ribs, scapula, and skull. However, scintigraphy has some substantial limitations, including exposure to ionizing radiation, difficulty in differentiating degenerative disease, and healing fractures from metastases. MRI has a unique detection rate for osseous metastases in the spine and the pelvis and was found to be definitely superior to skeletal scintigraphy.

To justify the higher costs of whole-body MRI, the range of diagnostic capabilities must be broad. Imaging must be performed to detect not only osseous metastases but also metastases in all other organ systems and tumor recurrences after regional therapy. This may be accomplished with T1w 3D-GRE with nearly isotropic resolution and gadolinium enhancement [24, 35]. Data are acquired within breath-hold periods, rendering image quality consistent. Good correlation with standard staging examinations including CT was observed. Dynamic imaging of the liver was accurate in the detection and characterization of hepatic mass lesions [42]. Other abdominal organs, including the pancreas, adrenal glands, and kidneys were imaged by MRI with a high level of diagnostic accuracy [25]. Lauenstein et al. [22] detected all cerebral and osseous metastases shown by the reference examinations. Image quality of the lungs proved to be slightly inferior to CT scanning. All pulmonary metastases except a single small lesion were correctly detected. These results were confirmed by other authors indicating that lesions larger than 5 mm in size can be adequately depicted with MRI [54]. A follow-up study which enrolled a larger patient cohort [23], comprising 51 patients with known malignant tumors, which all have the propensity to metastasize to different organ systems including brain, lungs, liver, lymph nodes, and bones. Reference staging was based on CT, dedicated MRI, and nuclear scintigraphy. In addition to gadolinium-enhanced T1w 3D GRE of the entire body, supplemental imaging of the thorax and abdomen was acquired with fat-suppressed T2-weighted (T2w) single-shot echo-train spin-echo. All 43 patients who were proven to have metastatic disease were found to have metastases on whole-body MRI. However, the reference examinations revealed metastatic disease in 42 patients only. In one patient with a single hepatic metastasis, which was proved by histology, only whole-body MRI was able to depict this lesion. There were distinct differences in the sensitivity of metastases detection depending on the anatomical region. More liver metastases were shown on MRI than on CT. Whole-body MRI did not reveal some lung lesions detected by CT. The addition of T2w sequences to a protocol employing only gadolinium-enhanced 3D-GRE images may improve the diagnostic information in lung involvement.

In another study comprising 98 patients, whole-body MRI was compared to dual-modality FDG-PET-CT in patients with a variety of malignancies [1]. Both modalities showed high accuracy using TNM staging

(77% PET-CT versus 54% with whole-body MRI). The extent of primary tumors and lymph nodes metastases was more reliably staged with PET-CT, while whole-body MRI was more sensitive and specific in the detection of hepatic and skeletal lesions. PET-CT performed particularly well in staging patients with primary lung cancer, which was the largest group in this study, reflecting the well established utility of PET/CT in patients with lung cancer.

The recent hardware developments of multiple phased-array surface coils and receiver channels combined with parallel imaging offer considerable reduction in data acquisition times, thereby permitting acquisition of a variety of sequences while maintaining acceptable study times.

Using these new techniques, the data published by Schmidt et al. [40] revealed distinctly better results and indicate that the tumor-stage can be as reliably assessed with whole-body MRI as with PET-CT. Both modalities showed high accuracy in TNM staging (96% PET-CT versus 91% with whole-body MRI). PET-CT achieved a diagnostic sensitivity and specificity of 82% for the detection of distant metastases, whereas whole-body MRI showed a sensitivity of 96% and a specificity of 82%. Whole-body MRI proved more reliable in the detection of skeletal and liver metastases by revealing 76 compared with 50 bone manifestations in PET-CT and 71 versus 62 liver manifestations, respectively (Fig. 9.2). The cutoff value for lesion detection in the liver was lower in MRI compared to PET-CT (3 mm versus 5 mm, respectively). PET-CT enabled the detection of more lung metastases and was also more accurate in the detection of soft tissue metastases. The option of implementing a dynamic MRI scan with PAT acceleration including contrast enhanced imaging, obviously contributed to a high detection rate and accurate evaluation of liver tumors [40].


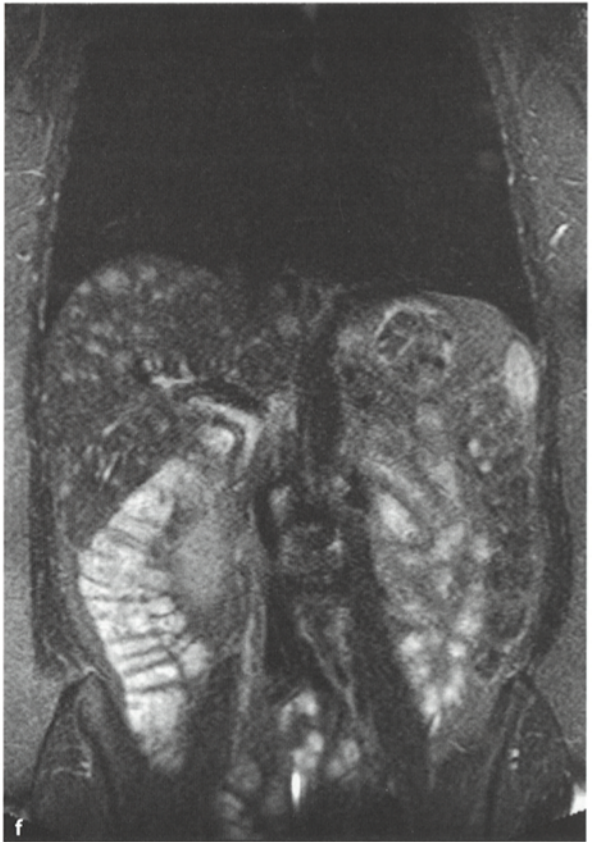
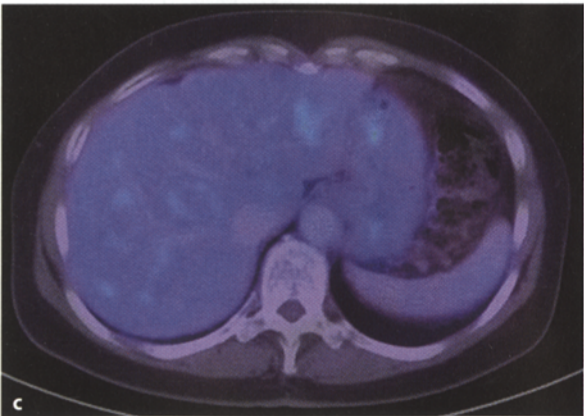
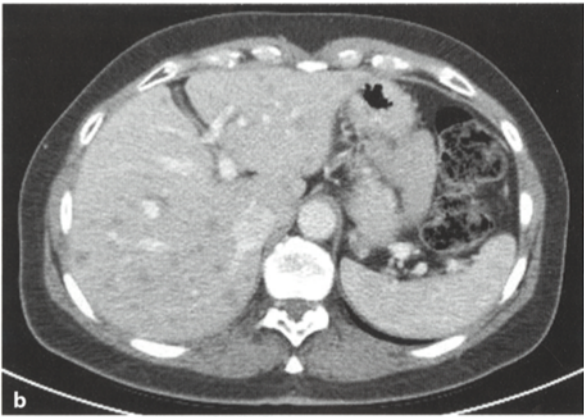
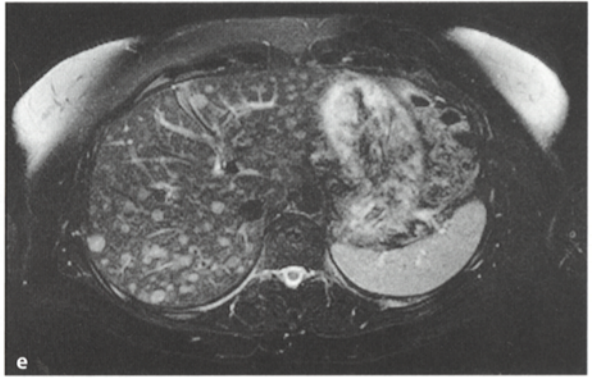
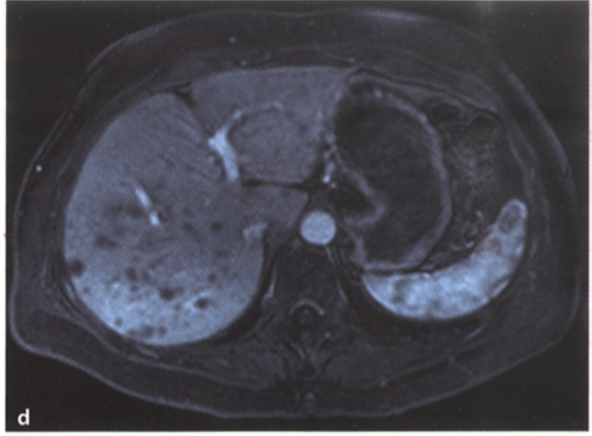
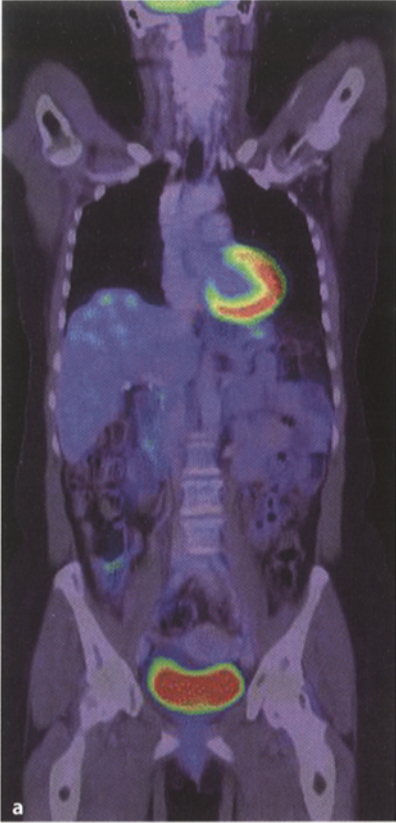


Fig. 9.2a-f. A 55-year-old female patient with hepatic metastases from breast cancer. The coronal (a) and axial (c) view of the fused PET-CT demonstrate only very few liver lesions with a high FDG-uptake. The contrast enhanced CT image (b) delineates some more hypodense liver lesions, which are apparently too small for the detection of an increased tumor metabolism. However, the T1w 3D-GRE with nearly isotropic resolution and gadolinium enhancement (d), as well as the T2w fat-saturated turbo spin-echo image (e) and the coronal STIR image (f) detect more metastases than PET-CT. Therefore, MRT with dedicated sequences is superior to PET-CT in the detection of smaller liver metastases. Especially in PET-negative tumors this is of special interest



Schlemmer et al. [39] analyzed the diagnostic performance of a multi-channel whole-body MRI scanner with the use of PAT in 71 patients with oncological diseases in comparison to conventional CT imaging. The protocol employed in this study was based on coronal STIR and axial pre- and post-contrast T1-weighted imaging of the whole body. Whole-body MRI showed promising performance for the detection of distant metastatic disease by revealing more metastases to the brain, abdominal organs, bone marrow and soft tissue in 17% of the patients. In six patients, therapy was modified according to these findings.

The presence of cerebral metastases, knowledge of which is crucial for patient management and prognosis, are usually not assessable in FDG-PET-CT due to the normal high FDG uptake in the cerebrum when a whole-body protocol is used. Cerebral pathologies are imaged with high resolution in whole-body MRI which is a clear advantage of this modality, especially in tumors that frequently spread to the brain, like breast carcinoma or bronchial carcinoma. In summary, whole-body MRI using T2w and contrast-enhanced T1w imaging includes all properties needed for detection of metastases: it is fast, provides high-quality MR data, and allows reliable detection of metastatic disease in various organ systems.

9.5

Outlook

Early detection of the response of hepatocellular carcinoma (HCC) to ^{90}Y microsphere brachytherapy may be important to permit repeat radioembolization or to alter treatment strategies. Water-mobility measurements with use of diffusion-weighted MRI appear useful for noninvasive interrogation of microstructural tissue properties. Findings of diffusion-weighted MRI may serve as an early biomarker of HCC response and represents a promising technique for non-invasive assessment of tumor response after radioembolization [11].

Potentially a so-called MRI-diffusion-PETgraphy described by Takahara et al. [45] may facilitate diagnosis of metastatic lymph node disease with the use of STIR-EPI-diffusion-sequences. The authors demonstrated pathological lymph nodes at high resolution and adequate fat suppression as a promising application in whole-body MRI.

9.6

Conclusion

Today, PET has an important role in the management of patients with liver metastases from various primaries. It provides functional information that can be used to detect hepatic metastases, to predict their response to therapy, and to follow-up them effectively. PET-CT has the unique advantage of combining functional and anatomic imaging in an integrated scanner and allows for a comprehensive evaluation of patients with liver metastases.

Both whole-body MRI and PET-CT are promising modalities for diagnostics in the oncological patient and seem suitable for accurate tumor staging and may replace extensive and costly multimodality diagnostics. Both modalities have particular diagnostic strengths and weaknesses: whilst PET-CT is superior in lymph node detection and assessment of tumor viability after regional therapy, high resolution MRI with the use of PAT represent a promising alternative. Particularly in the staging of tumors with known poor FDG uptake, like renal cell carcinoma or hepatocellular carcinoma, and of tumors with frequent metastatic spread to the bone, liver or CNS (e.g. breast cancer), whole-body MRI may represent an attractive alternative to PET-CT.

References

1. Antoch G, Vogt FM, Freudenberg LS, Nazaradeh F, Goehde SC, Barkhausen J, Dahmen G, Bockisch A, Debatin JF, Ruehm SG (2003) Whole-body dual-modality PET-CT and whole-body MRI for tumor staging in oncology. *Jama* 290:3199–3206
2. Arulampalam TH, Francis DL, Visvikis D, Taylor I, Ell PJ (2004) FDG-PET for the pre-operative evaluation of colorectal liver metastases. *Eur J Surg Oncol* 30:286–291
3. Barker DW, Zagoria RJ, Morton KA, Kavanagh PV, Shen P (2005) Evaluation of liver metastases after radiofrequency ablation: utility of ^{18}F -FDG PET and PET-CT. *AJR Am J Roentgenol* 184:1096–1102
4. Barkhausen J, Quick HH, Lauenstein T, Goyen M, Ruehm SG, Laub G, Debatin JF, Ladd ME (2001) Whole-body MR imaging in 30 seconds with real-time true FISP and a continuously rolling table platform: feasibility study. *Radiology* 220:252–256
5. Belton AL, Saini S, Liebermann K, Boland GW, Halpern EF (2003) Tumour size measurement in an oncology clinical trial: comparison between off-site and on-site measurements. *Clin Radiol* 58:311–314
6. Beyer T, Townsend DW, Brun T, Kinahan PE, Charron M, Roddy R, Jerin J, Young J, Byars L, Nutt R (2000) A com-

- bined PET-CT scanner for clinical oncology. *J Nucl Med* 41:1369-1379
7. Bohm B, Voth M, Geoghegan J, Hellfritsch H, Petrovich A, Scheele J, Gottschild D (2004) Impact of positron emission tomography on strategy in liver resection for primary and secondary liver tumors. *J Cancer Res Clin Oncol* 130:266-272
 8. Cohade C, Osman M, Leal J, Wahl RL (2003) Direct comparison of (¹⁸F)-FDG PET and PET-CT in patients with colorectal carcinoma. *J Nucl Med* 44:1797-1803
 9. Delbeke D, Vitola JV, Sandler MP, Arildsen RC, Powers TA, Wright JK Jr, Chapman WC, Pinson CW (1997) Staging recurrent metastatic colorectal carcinoma with PET. *J Nucl Med* 38:1196-1201
 10. Delbeke D, Martin WH (2004) PET and PET-CT for evaluation of colorectal carcinoma. *Semin Nucl Med* 34:209-223
 11. Deng J, Miller FH, Rhee TK, Sato KT, Mulcahy MF, Kulik LM, Salem R, Omary RA, Larson AC (2006) Diffusion-weighted MR imaging for determination of hepatocellular carcinoma response to yttrium-90 radioembolization. *J Vasc Interv Radiol* 17:1195-1200
 12. Eustace S, Tello R, DeCarvalho V, Carey J, Wroblecka JT, Melhem ER, Yucel EK (1997) A comparison of whole-body turboSTIR MR imaging and planar ^{99m}Tc-methylene diphosphonate scintigraphy in the examination of patients with suspected skeletal metastases. *AJR Am J Roentgenol* 169:1655-1661
 13. Fernandez FG, Drebin JA, Linehan DC, Dehdashti F, Siegel BA, Strasberg SM (2004) Five-year survival after resection of hepatic metastases from colorectal cancer in patients screened by positron emission tomography with F-18 fluorodeoxyglucose (FDG-PET). *Ann Surg* 240:438-447; discussion 447-450
 14. Griswold MA, Jakob PM, Heidemann RM, Nittka M, Jellus V, Wang J, Kiefer B, Haase A (2002) Generalized autocalibrating partially parallel acquisitions (GRAPPA). *Magn Reson Med* 47:1202-1210
 15. James K, Eisenhauer E, Christian M, Terenziani M, Vena D, Muldal A, Therasse P (1999) Measuring response in solid tumors: unidimensional versus bidimensional measurement. *J Natl Cancer Inst* 91:523-528
 16. Kamel IR, Bluemke DA (2002) Magnetic resonance imaging of the liver: assessing response to treatment. *Top Magn Reson Imaging* 13:191-200
 17. Kapoor V, McCook BM, Torok FS (2004) An introduction to PET-CT imaging. *Radiographics* 24:523-543
 18. Kinkel K, Lu Y, Both M, Warren RS, Thoeni RF (2002) Detection of hepatic metastases from cancers of the gastrointestinal tract by using noninvasive imaging methods (US, CT, MR imaging, PET): a meta-analysis. *Radiology* 224:748-756
 19. Kramer H, Schoenberg SO, Nikolaou K, Huber A, Struwe A, Winnik E, Wintersperger BJ, Dietrich O, Kiefer B, Reiser MF (2005) Cardiovascular screening with parallel imaging techniques and a whole-body MR imager. *Radiology* 236:300-310
 20. Langenhoff BS, Oyen WJ, Jager GJ, Strijk SP, Wobbes T, Corstens FH, Ruers TJ (2002) Efficacy of fluorine-18-deoxyglucose positron emission tomography in detecting tumor recurrence after local ablative therapy for liver metastases: a prospective study. *J Clin Oncol* 20:4453-4458
 21. Lardinois D, Weder W, Hany TF, Kamel EM, Korom S, Seifert B, von Schulthess GK, Steinert HC (2003) Staging of non-small-cell lung cancer with integrated positron-emission tomography and computed tomography. *N Engl J Med* 348:2500-2507
 22. Lauenstein TC, Goehde SC, Herborn CU, Treder W, Ruehm SG, Debatin JF, Barkhausen J (2002) Three-dimensional volumetric interpolated breath-hold MR imaging for whole-body tumor staging in less than 15 minutes: a feasibility study. *AJR Am J Roentgenol* 179:445-449
 23. Lauenstein TC, Goehde SC, Herborn CU, Goyen M, Oberhoff C, Debatin JF, Ruehm SG, Barkhausen J (2004) Whole-body MR imaging: evaluation of patients for metastases. *Radiology* 233:139-148
 24. Lee VS, Lavelle MT, Rofsky NM, Laub G, Thomasson DM, Krinsky GA, Weinreb JC (2000) Hepatic MR imaging with a dynamic contrast-enhanced isotropic volumetric interpolated breath-hold examination: feasibility, reproducibility, and technical quality. *Radiology* 215:365-372
 25. Low RN, Semelka RC, Worawattanakul S, Alzate GD (2000) Extrahepatic abdominal imaging in patients with malignancy: comparison of MR imaging and helical CT in 164 patients. *J Magn Reson Imaging* 12:269-277
 26. Mazumdar M, Smith A, Schwartz LH (2004) A statistical simulation study finds discordance between WHO criteria and RECIST guideline. *J Clin Epidemiol* 57:358-365
 27. Meta J, Seltzer M, Schiepers C, Silverman DH, Ariannejad M, Gambhir SS, Phelps ME, Valk P, Czernin J (2001) Impact of ¹⁸F-FDG PET on managing patients with colorectal cancer: the referring physician's perspective. *J Nucl Med* 42:586-590
 28. Miller AB, Hoogstraten B, Staquet M, Winkler A (1981) Reporting results of cancer treatment. *Cancer* 47:207-214
 29. Nelson RC, Chezmar JL, Sugarbaker PH, Bernardino ME (1989) Hepatic tumors: comparison of CT during arterial portography, delayed CT, and MR imaging for preoperative evaluation. *Radiology* 172:27-34
 30. Ogunbiyi OA, Flanagan FL, Dehdashti F, Siegel BA, Trask DD, Birnbaum EH, Fleshman JW, Read TE, Philpott GW, Kodner IJ (1997) Detection of recurrent and metastatic colorectal cancer: comparison of positron emission tomography and computed tomography. *Ann Surg Oncol* 4:613-620
 31. Park JO, Lee SI, Song SY, Kim K, Kim WS, Jung CW, Park YS, Im YH, Kang WK, Lee MH, Lee KS, Park K (2003) Measuring response in solid tumors: comparison of RECIST and WHO response criteria. *Jpn J Clin Oncol* 33:533-537
 32. Pelosi E, Messa C, Sironi S, Picchio M, Landoni C, Bettinardi V, Gianolli L, Del Maschio A, Gilardi MC, Fazio F (2004) Value of integrated PET-CT for lesion localisation in cancer patients: a comparative study. *Eur J Nucl Med Mol Imaging* 31:932-939
 33. Pfannenberger C, Aschoff P, Schanz S, Eschmann SM, Plathow C, Eigentler TK, Garbe C, Brechtel K, Vonthein R, Bares R, Claussen CD, Schlemmer HP (2007) Prospective comparison of (¹⁸F)-fluorodeoxyglucose positron emission tomography/computed tomography and whole-body magnetic resonance imaging in staging of advanced malignant melanoma. *Eur J Cancer* 43:557-564
 34. Pruessmann KP, Weiger M, Scheidegger MB, Boesiger P (1999) SENSE: sensitivity encoding for fast MRI. *Magn Reson Med* 42:952-962

35. Rofsky NM, Lee VS, Laub G, Pollack MA, Krinsky GA, Thomasson D, Ambrosino MM, Weinreb JC (1999) Abdominal MR imaging with a volumetric interpolated breath-hold examination. *Radiology* 212:876–884
36. Rohren EM, Paulson EK, Hagge R, Wong TZ, Killius J, Clavien PA, Nelson RC (2002) The role of F-18 FDG positron emission tomography in preoperative assessment of the liver in patients being considered for curative resection of hepatic metastases from colorectal cancer. *Clin Nucl Med* 27:550–555
37. Ruers TJ, Langenhoff BS, Neeleman N, Jager GJ, Strijk S, Wobbes T, Corstens FH, Oyen WJ (2002) Value of positron emission tomography with [F-18]fluorodeoxyglucose in patients with colorectal liver metastases: a prospective study. *J Clin Oncol* 20:388–395
38. Sahani DV, Kalva SP, Fischman AJ, Kadavigere R, Blake M, Hahn PF, Saini S (2005) Detection of liver metastases from adenocarcinoma of the colon and pancreas: comparison of mangafodipir trisodium-enhanced liver MRI and whole-body FDG PET. *AJR Am J Roentgenol* 185:239–246
39. Schlemmer HP, Schafer J, Pfannenbergl C, Radny P, Korchidi S, Muller-Horvat C, Nagele T, Tomaschko K, Fenchel M, Claussen CD (2005) Fast whole-body assessment of metastatic disease using a novel magnetic resonance imaging system: initial experiences. *Invest Radiol* 40:64–71
40. Schmidt GP, Baur-Melnyk A, Herzog P, Schmid R, Tiling R, Schmidt M, Reiser MF, Schoenberg SO (2005) High-resolution whole-body magnetic resonance image tumor staging with the use of parallel imaging versus dual-modality positron emission tomography-computed tomography: experience on a 32-channel system. *Invest Radiol* 40:743–753
41. Selzner M, Hany TF, Wildbrett P, McCormack L, Kadry Z, Clavien PA (2004) Does the novel PET-CT imaging modality impact on the treatment of patients with metastatic colorectal cancer of the liver? *Ann Surg* 240:1027–1034; discussion 1035–1036
42. Semelka RC, Martin DR, Balci C, Lance T (2001) Focal liver lesions: comparison of dual-phase CT and multisequence multiplanar MR imaging including dynamic gadolinium enhancement. *J Magn Reson Imaging* 13:397–401
43. Soyer P, Levesque M, Elias D, Zeitoun G, Roche A (1992) Detection of liver metastases from colorectal cancer: comparison of intraoperative US and CT during arterial portography. *Radiology* 183:541–544
44. Steinborn MM, Heuck AF, Tiling R, Bruegel M, Gauger L, Reiser MF (1999) Whole-body bone marrow MRI in patients with metastatic disease to the skeletal system. *J Comput Assist Tomogr* 23:123–129
45. Takahara T, Imai Y, Yamashita T, Yasuda S, Nasu S, Van Cauteren M (2004) Diffusion weighted whole body imaging with background body signal suppression (DWIBS): technical improvement using free breathing, STIR and high resolution 3D display. *Radiat Med* 22:275–282
46. Therasse P, Arbuck SG, Eisenhauer EA, Wanders J, Kaplan RS, Rubinstein L, Verweij J, Van Glabbeke M, van Oosterom AT, Christian MC, Gwyther SG (2000) New guidelines to evaluate the response to treatment in solid tumors. European Organization for Research and Treatment of Cancer, National Cancer Institute of the United States, National Cancer Institute of Canada. *J Natl Cancer Inst* 92:205–216
47. Topal B, Flamen P, Aerts R, D’Hoore A, Filez L, Van Cutsem E, Mortelmans L, Penninckx F (2001) Clinical value of whole-body emission tomography in potentially curable colorectal liver metastases. *Eur J Surg Oncol* 27:175–179
48. Torizuka T, Tamaki N, Inokuma T, Magata Y, Yonekura Y, Tanaka A, Yamaoka Y, Yamamoto K, Konishi J (1994) Value of fluorine-18-FDG-PET to monitor hepatocellular carcinoma after interventional therapy. *J Nucl Med* 35:1965–1969
49. Tran LN, Brown MS, Goldin JG, Yan X, Pais RC, McNitt-Gray MF, Gjertson D, Rogers SR, Aberle DR (2004) Comparison of treatment response classifications between unidimensional, bidimensional, and volumetric measurements of metastatic lung lesions on chest computed tomography. *Acad Radiol* 11:1355–1360
50. Truant S, Huglo D, Hebbbar M, Ernst O, Steinling M, Pruvot FR (2005) Prospective evaluation of the impact of [18F]fluoro-2-deoxy-D-glucose positron emission tomography of resectable colorectal liver metastases. *Br J Surg* 92:362–369
51. Tutt AN, Plunkett TA, Barrington SF, Leslie MD (2004) The role of positron emission tomography in the management of colorectal cancer. *Colorectal Dis* 6:2–9
52. Valk PE, Abella-Columna E, Haseman MK, Pounds TR, Tesar RD, Myers RW, Greiss HB, Hofer GA (1999) Whole-body PET imaging with [18F]fluorodeoxyglucose in management of recurrent colorectal cancer. *Arch Surg* 134:503–511; discussion 511–513
53. Vitola JV, Delbeke D, Meranze SG, Mazer MJ, Pinson CW (1996) Positron emission tomography with F-18-fluorodeoxyglucose to evaluate the results of hepatic chemoembolization. *Cancer* 78:2216–2222
54. Vogt FM, Herborn CU, Hunold P, Lauenstein TC, Schroder T, Debatin JF, Barkhausen J (2004) HASTE MRI versus chest radiography in the detection of pulmonary nodules: comparison with MDCT. *AJR Am J Roentgenol* 183:71–78
55. Wong CY, Salem R, Raman S, Gates VL, Dworkin HJ (2002) Evaluating ⁹⁰Y-glass microsphere treatment response of unresectable colorectal liver metastases by [18F]FDG PET: a comparison with CT or MRI. *Eur J Nucl Med Mol Imaging* 29:815–820
56. Wong CY, Salem R, Qing F, Wong KT, Barker D, Gates V, Lewandowski R, Hill EA, Dworkin HJ, Nagle C (2004) Metabolic response after intraarterial ⁹⁰Y-glass microsphere treatment for colorectal liver metastases: comparison of quantitative and visual analyses by ¹⁸F-FDG PET. *J Nucl Med* 45:1892–1897
57. Wong CY, Qing F, Savin M, Campbell J, Gates VL, Sherpa KM, Lewandowski RJ, Nagle C, Salem R (2005) Reduction of metastatic load to liver after intraarterial hepatic yttrium-90 radioembolization as evaluated by [18F]fluorodeoxyglucose positron emission tomographic imaging. *J Vasc Interv Radiol* 16:1101–1106
58. Yang M, Martin DR, Karabulut N, Frick MP (2003) Comparison of MR and PET imaging for the evaluation of liver metastases. *J Magn Reson Imaging* 17:343–349